



**HAL**  
open science

# Light-response in two clonal strains of the haptophyte *Tisochrysis lutea*: Evidence for different photoprotection strategies

Anne Pajot, Johann Lavaud, Gregory Carrier, Thomas Lacour, Luc Marchal,  
Elodie Nicolau

## ► To cite this version:

Anne Pajot, Johann Lavaud, Gregory Carrier, Thomas Lacour, Luc Marchal, et al.. Light-response in two clonal strains of the haptophyte *Tisochrysis lutea*: Evidence for different photoprotection strategies. *Algal Research - Biomass, Biofuels and Bioproducts*, 2023, 69, pp.102915. 10.1016/j.algal.2022.102915 . hal-03920326

**HAL Id: hal-03920326**

**<https://hal.science/hal-03920326>**

Submitted on 3 Jan 2023

**HAL** is a multi-disciplinary open access archive for the deposit and dissemination of scientific research documents, whether they are published or not. The documents may come from teaching and research institutions in France or abroad, or from public or private research centers.

L'archive ouverte pluridisciplinaire **HAL**, est destinée au dépôt et à la diffusion de documents scientifiques de niveau recherche, publiés ou non, émanant des établissements d'enseignement et de recherche français ou étrangers, des laboratoires publics ou privés.

1 **Light-response in two clonal strains of the haptophyte *Tisochrysis lutea*: evidence for**  
2 **different photoprotection strategies.**

3 Anne Pajot<sup>1</sup>, Johann Lavaud<sup>2</sup>, Gregory Carrier<sup>3</sup>, Thomas Lacour<sup>3</sup>, Luc Marchal<sup>4</sup>, Elodie  
4 Nicolau<sup>1</sup>.

5

6 <sup>1</sup> Ifremer, PHYTOX, GENALG Laboratory, F-44000 Nantes, France

7 <sup>2</sup> LEMAR, Laboratory of Marine Environmental Sciences, UMR 6539, CNRS/Univ  
8 Brest/Ifremer/IRD, Institut Universitaire Européen de la Mer, Technopôle Brest-Iroise,  
9 Plouzané, France

10 <sup>3</sup> Ifremer, PHYTOX, PHYSALG Laboratory, F-44000 Nantes, France

11 <sup>4</sup> Université de Nantes, GEPEA, F-44000 Saint Nazaire, France

12

13 Corresponding author:

14 Anne Pajot

15 Tel: +33 2 40 37 40 66

16 Email: [anne.pajot@gmail.com](mailto:anne.pajot@gmail.com)

17 Permanent adress: Ifremer, rue de l'Île d'Yeu, 44000, - Nantes, France

18

19

20 **Abstract**

21 To assess the mechanisms of photoprotection in *T. lutea*, two clonal strains with different basal  
22 pigments composition were studied. One synthesized echinenone, while the other did not but  
23 showed a high amount of diadinoxanthin and diatoxanthin.

24 We investigated the photosynthetic response of these two clonal strains in turbidostat, at  
25 different growth culture irradiances from 50 to 550  $\mu\text{mol photons m}^2 \text{s}^{-1}$ . To this end, variable  
26 chlorophyll *a* fluorescence, pigment composition and transcription level of specific genes were  
27 monitored. In addition to the genes coding for the Fucoxanthin Chlorophyll *a, c* binding Protein  
28 (FCP), we followed the expression of several putative genes coding for the diadinoxanthin de-  
29 epoxidase, the violaxanthin de-epoxidase and the zeaxanthin epoxidase enzymes. It was the  
30 first time that these genes were characterized in *T. lutea*.

31 Both clonal strains decreased their photosynthetic pigments with increasing irradiance.  
32 Nevertheless, the two clonal strains had different photoprotection strategies illustrated with the  
33 extent of the dissipation of excess light energy. It was accompanied by the synthesis of  
34 photoprotective pigments to different extents: T-5cl6 increased its pool of diadinoxanthin-  
35 diatoxanthin with increasing irradiance, while T 4cl3 preferentially synthesized echinenone  
36 above a certain level of irradiance. These diverging phenotypes were correlated with variations  
37 in the expression of *lhcx*, *lhcr*, and of the putative genes of the enzymes involved in the  
38 xanthophyll pigment cycles.

39

40 **Keywords**

41 *Tisochrysis lutea*, photoprotection, diatoxanthin, zeaxanthin, echinenone, *lhcx*

42

43 **Abbreviations**

44 ROS: reactive oxygen species

45 LHC: light-harvesting complex

46 FCP: Fucoxanthin Chlorophyll *a,c* binding Protein

47 PPF: photosynthetic photon flux,  $\mu\text{mol photons m}^2 \text{s}^{-1}$

48 Ddx: diadinoxanthin

49 Dtx: diatoxanthin

50 Vx: violaxanthin

51 Zx: zeaxanthin

52 DDE: diadinoxanthin de-epoxidase

53 VDE: violaxanthin de-epoxidase

54 ZE: zeaxanthin epoxidase

55 NPQ: non-photochemical quenching

56 DES-DD: de-epoxidation state from diadinoxanthin to diatoxanthin

57 DES-VZ: de-epoxidation state from violaxanthin to zeaxanthin

58

## 59 1. Introduction

60 Chromista is a well-known clade responsible for 25% of the primary production on Earth [1],  
61 composed of brown seaweeds and microalgae, including diatoms and haptophytes. These latter  
62 groups are ubiquitous in oceans, and are able to cope with fluctuating light conditions. While  
63 performing photosynthesis for their growth, cells have to avoid the photodamages caused by an  
64 excess of light energy absorption, generating various reactive oxygen species (ROS) [2,3]. The  
65 achievement of an efficient balance between photosynthesis and photoprotection explains part  
66 of the worldwide expansion of diatoms and haptophytes [4–6], and they developed several  
67 strategies to achieve it. The major player of this very dynamic equilibrium is the light-  
68 harvesting antenna, also called the light-harvesting complex (LHC) [7].

69  
70 The LHC of diatoms and haptophytes, common to all Chromista, is composed of photosynthetic  
71 and photoprotective pigments, and of the Fucoxanthin Chlorophyll *a,c* binding Protein (FCP)  
72 [7]. The FCP is a thylakoid transmembrane protein complex composed of three main protein  
73 families. The Lhcf and Lhcr are protein sequences binding mostly photosynthetic pigments  
74 such as fucoxanthin (Fx) and chlorophylls (Chl *a* and *c*). The Lhcx bind mostly photoprotective  
75 pigments such as diadinoxanthin (Ddx), diatoxanthin (Dtx) [8–10]. It is therefore assumed that  
76 Lhcf and Lhcr are related to photosynthesis and Lhcx to photoprotection. However, Lhcf can  
77 also bind Ddx, for instance in the diatom *Phaeodactylum tricornutum* [11], highlighting the  
78 more complex role of Lhcf within the light-harvesting antenna. Currently in the literature, there  
79 is an abundance of studies on the FCP of diatoms [12,13], whereas only a few exist for  
80 haptophytes [14,15].

81  
82 We selected *Tisochrysis lutea* as a representative of haptophyte microalgae, and determined the  
83 composition of its FCP in a previous study [15]. 28 Lhcf, 12 Lhcr and 12 Lhcx protein  
84 sequences constitute the FCP of *T. lutea*, and at least five Fx molecules and nine Chl *a* and *c*  
85 molecules are bound to a majority of Lhcf monomers in this species [15]. In diatoms and  
86 haptophytes, a correlation was already established between the expression of the FCP and the  
87 concentration of pigments in cells. Especially, a clear correlation between the Lhcx and the  
88 photoprotective xanthophyll cycle Ddx-Dtx was observed in diatoms and haptophytes. In the  
89 diatom *Thalassiosira pseudonana*, both Dtx content and Lhcx proteins increased under high-  
90 light [9]. In *Phaeodactylum tricornutum*, the same correlation was observed between the Ddx-  
91 Dtx pool, three *lhcx* genes [10], and the Lhcx2 and Lhcx3 proteins [16,17]. In *T. lutea*, the

92 increase in Dtx was also correlated with the increase in *lhcx* genes expression under high light  
93 during a day:night cycle experiment [15].

94

95 Under high light conditions, Ddx and violaxanthin (Vx) are de-epoxidized into Dtx and Zx  
96 respectively. These reactions are driven by the diadinoxanthin de-epoxidase (DDE) and the  
97 violaxanthin de-epoxidase (VDE). Reverse reactions of epoxidation imply epoxidases, and take  
98 place at low light [18]. These enzymes are activated by the development of a light-driven proton  
99 gradient across the thylakoid membrane and an acidification of the thylakoid lumen [19].  
100 Contrary to the Ddx-Dtx cycle, well-known and well-described in diatoms and haptophytes, the  
101 Vx-Zx cycle is usually associated to higher plants and green algae only [20–22]. However, this  
102 cycle is also present in brown algae, in diatoms, where it prevents photoinhibition [23,24], and  
103 haptophytes such as *T. lutea*, as a secondary xanthophyll cycle [25,26]. Together with Lhcx  
104 proteins, both Ddx-Dtx and Vx-Zx cycles participate in the non-photochemical quenching  
105 (NPQ), more precisely the fast energy-dependent quenching (qE), which allows the dissipation,  
106 as heat, of excess excitation energy, induced by high irradiance [27]. In Chromista, models for  
107 NPQ measurement were established mainly for diatoms, and are not perfectly adapted to  
108 haptophytes, including *T. lutea* [28]. Indeed, the NPQ of *T. lutea* is sustained, which means  
109 NPQ is still present in darkness, *i.e.* its relaxation kinetics is not minutes but hours [29,30].  
110 Therefore, the usual NPQ measure is not reliable for *T. lutea*. To overcome this problem, and  
111 in order to evaluate the dynamics between photochemistry and photoprotection, the  
112 measurement of the dark relaxation of the maximum quantum yield of the PSII ( $F_v/F_m$ ) on  
113 steady-state photoacclimated microalgal cultures is required [29]. In these specific conditions,  
114 and as shown in diatoms,  $F_v/F_m$  is related to the NPQ extent and to the Dtx amount [29]

115

116 In this work, two clonal strains of *T. lutea* were selected for their different pigment composition.  
117 Indeed, it was previously observed that T-5cl6 accumulated more Dtx and Vx than T-4cl3, and  
118 that T-4cl3 produced 19 times more echinenone than T-5cl6 under N-deprivation condition  
119 (Pajot *et al.*, in prep.). The overall objective of this study was to understand how potentially  
120 different photoprotection strategies would be expressed in these two strains. Using turbidostat  
121 cultures, we examined in both strains the photoacclimative response (pigments and  
122 transcriptomics) and the extent of the dissipation of the excess light (dark  $F_v/F_m$  as a proxy for  
123 NPQ) as a function of increasing irradiance. The genes of interest we investigated were the  
124 genes coding for the light-harvesting antenna proteins (*lhcf*, *lhcx* and *lhcr*), and for the de-  
125 epoxidases and epoxidases involved in the xanthophyll pigment cycles (DDE, VDE, ZE).

126

## 127 **2. Materials and Methods**

### 128 **2.1. Culture conditions**

129 Experiments were performed with two *Tisochrysis lutea* clonal strains, T-5cl6 and T-4cl3,  
130 respectively clone 6 from strain Ifremer-Argenton, isolated in Atlantic Ocean near Argenton,  
131 France and clone 3 from strain RCC1344, isolated in Atlantic Ocean at the level of the spanish  
132 coast. These strains were polyclonal and the different clones have been isolated by flow  
133 cytometry (platform Cytocell, University of Nantes, France). Current analyses performed in the  
134 laboratory are demonstrating genetic polymorphism between the two strains, resulted in  
135 phenotypic differences at the pigments and lipids content level.

136

137 We set up an experiment to observe the physiological response of the two strains with varying  
138 growth irradiances. Inoculum were maintained in Walne's medium (Walne, 1966) at 150  $\mu\text{mol}$   
139  $\text{photons m}^{-2} \text{s}^{-1}$  (or PPF: Photosynthetic Photon Flux). The effect of different light irradiances  
140 (50, 150, 300 and 550  $\mu\text{mol photons m}^{-2} \text{s}^{-1}$ ) was determined for each strain in continuous 3.5  
141 L photobioreactors (PBR). These PBR were made of two transparent polymethylmetacrylate  
142 (PMMA) columns (60 mm diameter) connected by two flanges (for design reference, see the  
143 single module in Loubière *et al.*, 2009 [31]). Light was delivered by six dimmable fluorescent  
144 white tubes. It was measured outside the PBR, at middle height between the two columns, using  
145 a spherical quantum sensor (LI-250 light meter, LI-COR, 3mm diameter).

146

147 Cultures were constantly aerated and thermoregulated at  $26 \pm 1^\circ\text{C}$  by air conditioning and water  
148 circuit. pH was maintained constant at 8.2 with automatic injections of  $\text{CO}_2$ , measured with a  
149 pH measurement loop (electrode Inpro 4800/225/PT1000, Mettler Toledo and HPT 63, LTH  
150 electronics Ltd). Walne's medium enriched sea water ( $1 \text{ mL L}^{-1}$ ) was provided automatically  
151 by a metering pump (Simdos®) in order to maintain the culture at constant turbidity, *i.e.* at  
152 constant cell concentration. The excess culture was eliminated through an overflow pipe into a  
153 container. Cultures were monitored by a sensor to be maintained at low turbidity, between  $1.5$   
154 and  $2.5 \cdot 10^6 \text{ cells mL}^{-1}$  (Fig. S4) in order to reduce self-shading and therefore keep the optical  
155 properties of the cultures stable. Each experiment was conducted in triplicate. Small error bars  
156 confirm the relevance of the three replicates in validating the biological data (Fig. S4). Cultures  
157 were maintained seven to ten days at each light irradiance before sampling, in order for cells to  
158 acclimate and cultures to be at the equilibrium, *i.e.* at a steady-state. Cultures were assumed to  
159 be at steady-state when Chl *a* content was stable for at least three consecutive days with less

160 than 10 % variation (Fig. S5, S6). In total, the experiment lasted four to five weeks per clonal  
161 strain.

162

### 163 **2.2. Chl a, cell concentration monitoring and growth rate**

164 To measure the Chl *a* content, cells were harvested daily from 10 mL of culture on a 0.2  $\mu$ m  
165 fiberglass filter, and immediately immersed in 1.5 mL 95% acetone, during 24 hours.  
166 Absorbance was measured at 665 and 750 nm, before and after acidification with HCl 0.3 M.  
167 The number of cells per mL of culture (cell concentration, Fig. S4) was measured on a  
168 Multisizer Counter Coulter (Beckman Coulter®). Growth rate ( $\mu$ ) was measured daily by  
169 weighing the excess culture in the overflow container, which represented the daily dilution rate  
170 of the culture (Fig. S4).

171

### 172 **2.3. Pigment extraction and HPLC analysis**

173 Cell pigment content (Chl *a* in pg cell<sup>-1</sup>, Fx, Ddx, Dtx and echinenone in mol(100 mol Chl *a*)<sup>-1</sup>  
174 was measured after seven to ten days at each light irradiance (50, 150, 300 and 550 PPF). Cells  
175 were harvested on a 0.2  $\mu$ m fiberglass filter (GF/F, Whatman™) and immediately stored at -  
176 80°C. Four weeks later, they were immersed in 2 mL of 95% acetone, subjected to an ultrasonic  
177 bath for 10 minutes, and placed at -20°C overnight. The acetone extracts were filtered on a 0.2  
178  $\mu$ m fiberglass filter prior to injection in HPLC. The filtered acetone extracts were analyzed by  
179 HPLC-UV-DAD (Agilent Technologies series 1200 HPLC-UV-DAD) using an Eclipse XDB-  
180 C8 reverse phase column (150 x 4.6 mm, 3.5  $\mu$ m particle size, Agilent) following the method  
181 described by Van Heukelem & Thomas (2001) [32] with slight modifications. Briefly, solvent  
182 A was 70:30 MeOH: H<sub>2</sub>O 28 mM ammonium acetate and solvent B was pure MeOH (Merck  
183 France). Gradient elution was the same as described in Van Heukelem & Thomas (2001) [32].  
184 Quantification was carried out using external calibration against pigment standards (DHI,  
185 Denmark).

186

### 187 **2.4. Chlorophyll fluorescence measurement**

188 At steady-state, the triplicate culture subsamples acclimated to each growth irradiance were  
189 harvested. In parallel with pigment content, the chlorophyll fluorescence was measured with a  
190 PHYTO-PAM (WALZ). The effective PSII quantum yield in the dark ( $F_v/F_m$ ) was measured  
191 immediately after sampling, and following 15 min, 1 h and 2 h of dark acclimation, and  
192 calculated as:



193

$$F_v/F_m = \frac{F_m - F_0}{F_m}$$

194 With  $F_0$  and  $F_m$  the minimal and maximal fluorescence respectively.

195

196 **2.5. RNAseq**

197 At the steady-state, 50 mL of triplicate cultures acclimated to each growth irradiance were  
 198 sampled for transcriptomic analysis. After centrifugation (10 min, 8000 g), total RNA was  
 199 extracted from each strain (T-5cl6 and T-4cl3) using the TRIZOL reagent (Invitrogen, USA)  
 200 according to the manufacturer's instructions. DNase treatment (DNase RQ1, Promega) was  
 201 used to remove residual genomic DNA. The quantity of purified total RNA was determined by  
 202 a Qubit 3 Fluorometer (Invitrogen, USA) using the AccuBlue® Broad Range RNA Quantitation  
 203 Kit (Biotium, USA). The quality of purified total RNA was determined by measurement of  
 204 absorbance (260 nm/280 nm) using a Nanodrop ND-1000 spectrophotometer (LabTech, USA).  
 205 Poly(A) mRNA were selected, libraries of RNAseq were built using bare code according to  
 206 Illumina's protocol. Sequencing was performed using the paired-ends method with an Illumina  
 207 NovaSeq sequencer by the GenoToul platform (INRAE, Toulouse, France). The read length  
 208 was 260 bases. Transcripts were normalized according to the median of ratio method proposed  
 209 by the DESeq2 package in R: counts were divided by sample-specific size factors determined  
 210 by the median ratio. The median ratio is the ratio of gene counts relative to geometric mean per  
 211 gene. Table 1 shows the average number of normalized transcripts for each strain at each growth  
 212 irradiance.

213

214 **Table 1:** Number of normalized reads for all growth irradiances for T-5cl6 and T-4cl3

	T-5cl6	T-4cl3
50 $\mu\text{mol m}^{-2}$	3.3E+07	2.6E+07
150 $\mu\text{mol m}^{-2}$	3.0E+07	2.5E+07
300 $\mu\text{mol m}^{-2}$	3.2E+07	3.7E+07
550 $\mu\text{mol m}^{-2}$	2.5E+07	2.8E+07

215

216 Raw reads of each sample were filtered using TrimGalore to remove known Illumina adapter  
 217 sequences. Low quality reads were excluded using a quality score threshold of 30 and a minimal  
 218 length of 75 or 150 bases. The quality of reads was assessed using FastQC. Then, sequenced  
 219 reads for each sample were aligned using HISAT2. Each gene within the alignment was counted

220 using the Rsubread package in R with the function featureCounts, based on *T. lutea* reference  
221 genome [33]. Gene counts were obtained for each sample and normalized with DESeq2.

222

## 223 **2.6. Similarity research**

224 We performed a similarity research using BLAST [34] between the annotated DDE, VDE, VDL  
225 (violaxanthin de-epoxidase like) and VDR (violaxanthin de-epoxidase related) of several  
226 diatoms and haptophytes and *T. lutea* genome (Table S1, S2). All targets were selected and the  
227 best BLAST scores were selected as putative genes in *T. lutea*. For diatoms, there were one  
228 DDE from *Thalassiosira pseudonana*, nine VDE domain-containing proteins from *Fistulifera*  
229 *solaris*, *Thalassiosira oceanica* and *Thalassiosira pseudonana*, six VDE from *Fragilariopsis*  
230 *cylindrus*, *Phaeodactylum tricornutum*, *F. solaris*, two VDL precursors from *P. tricornutum*,  
231 two VDL from *T. pseudonana*, one VDR from *P. tricornutum*. For haptophytes, there were five  
232 VDE from *Chrysochromulina tobinii* and *Emiliania huxleyi*, four VDE domain-containing  
233 proteins from *E. huxleyi*, and one VDL from *C. tobinii*. We also considered the reverse reaction  
234 of epoxidation. We found several zeaxanthin epoxidases (ZE and ZE like: ZEL) but no  
235 diatinoxanthin epoxidase was recorded in UniprotKB databases. In diatoms, there were nine ZE  
236 from *T. pseudonana*, *F. solaris*, *F. cylindrus*, *P. tricornutum* and one ZEL from *P. tricornutum*.  
237 In haptophytes, there were seven ZE from *C. tobinii* and *E. huxleyi*.

238

## 239 **2.7. Statistics**

240 For each average measure of the culture triplicates (pigment content and normalized transcript  
241 counts), we used a confidence interval, characterized by error bars on graphics, calculated at a  
242 95% confidence level:

$$243 \text{ Confidence interval} = Z_{\alpha/2} * \frac{sd}{\sqrt{(n)}}$$

244

245 With  $Z_{\alpha/2} = 1,96$ ,  $sd$  = standard deviation,  $n = 3$  (number of triplicates)

246 Statistical differences were calculated between T-5cl6 and T-4cl3. The p-values indicated in  
247 each figure is therefore representative of the difference between the two strains (except in Fig.  
248 6). At each irradiance, the dataset was made of three values, corresponding to the three culture  
249 replicates of T-5cl6 or T-4cl3. Therefore, a Student test was carried out first, and then an  
250 ANOVA test.

251

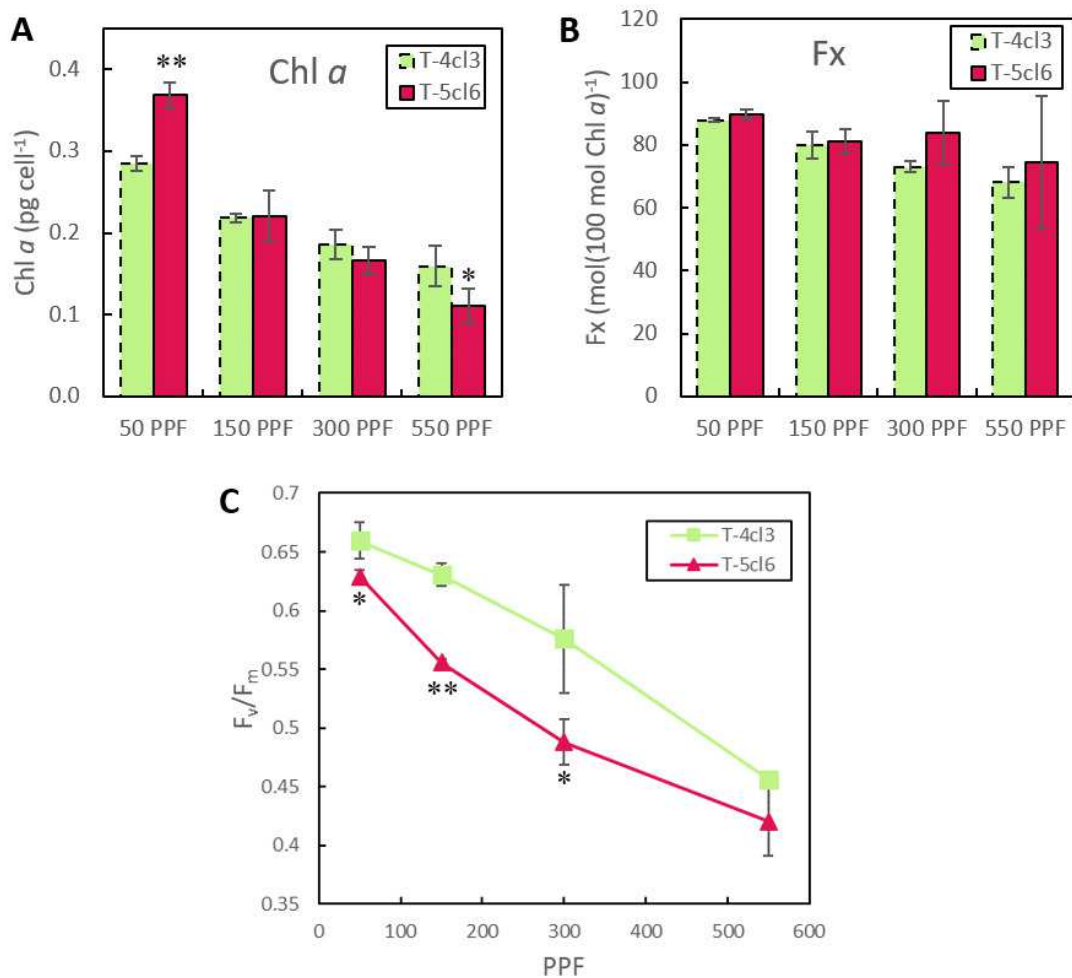
## 252 **3. Results**

253 **3.1. Photosynthetic pigments and photochemical properties**

254 Chl *a* content per cells gradually decreased with growth irradiance for both strains (Fig. 1A).  
 255 In both strains, Fx normalized by Chl *a* gradually decreased with growth irradiance (Fig. 1B).  
 256 At 50 PPF, T-5cl6 contained more Chl *a* than T-4cl3, and more Fx, as the Fx per Chl *a* ratio  
 257 was similar in both strains. At 550 PPF it was the contrary, T-5cl6 contained less Chl *a* than T-  
 258 4cl3.

259  
 260 In both strains,  $F_v/F_m$  decreased with the increase of growth irradiance (Fig. 1C). For all growth  
 261 irradiances,  $F_v/F_m$  in T-5cl6 was lower than in T-4cl3. The difference between the two strains  
 262 was the most significant at 150 PPF (pvalue < 0.01).

263



264  
 265 **Figure 1:** Evolution of the Chl *a* content (average  $\pm$  the confidence interval, pg cell<sup>-1</sup>) (A), of  
 266 the Fx content normalized by Chl *a* (average  $\pm$  the confidence interval, mol(100 mol Chl *a*)<sup>-1</sup>)  
 267 (B), of the maximum PSII quantum yield  $F_v/F_m$  (average  $\pm$  the confidence interval)  
 268 (C), relatively to growth irradiance (PPF = Photosynthetic Photon Flux =  $\mu\text{mol m}^2 \text{s}^{-1}$ ). \*: pvalue  
 269 < 0.05, \*\*: pvalue < 0.01. \*: pvalue < 0.05, \*\*: pvalue < 0.01.

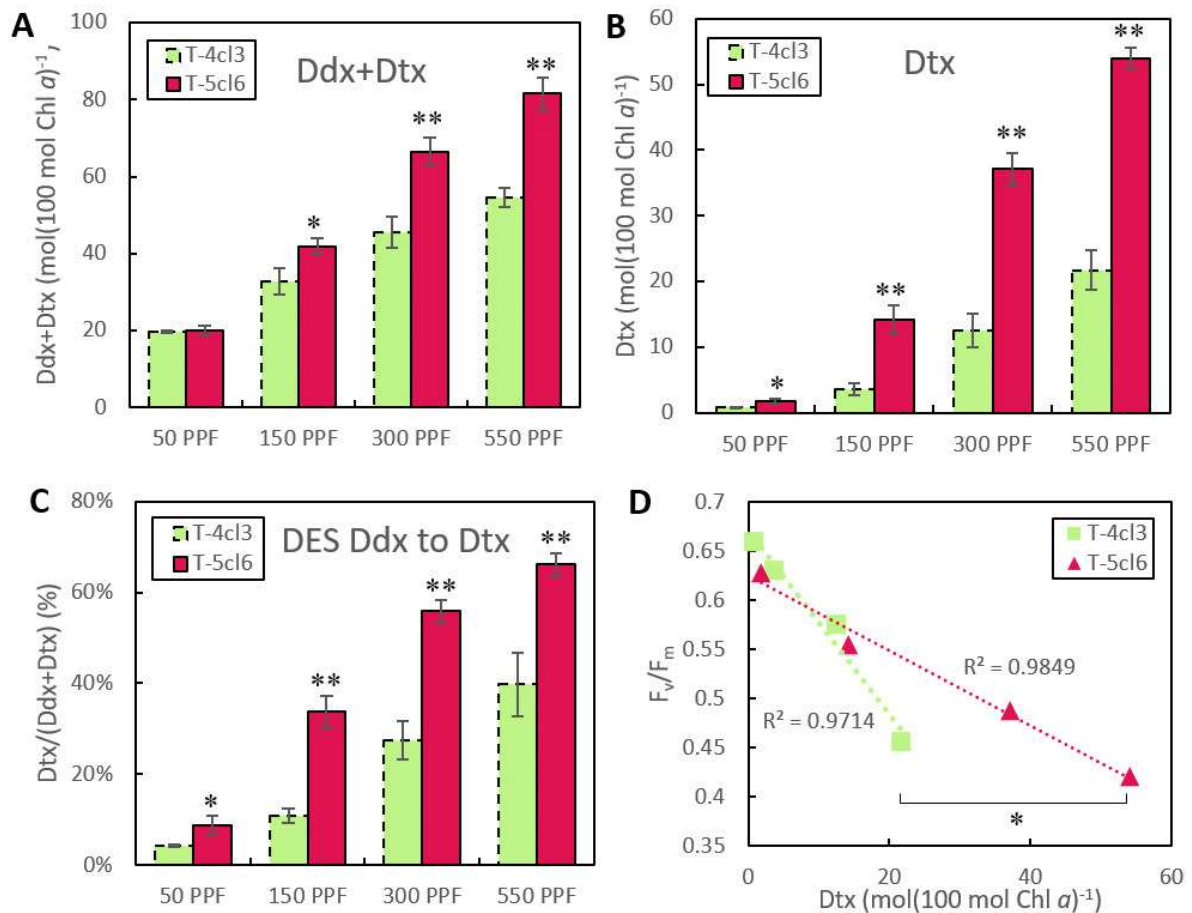
270

271 **3.2. Photoprotective pigments and  $F_v/F_m$**

272 With increasing growth irradiance, the Ddx+Dtx pool size increased 4-fold in T-5cl6 and 2.75-  
273 fold in T-4cl3 (Fig. 2A). The difference between the two strains was mainly explained by the  
274 highly variable values of Dtx amount (Fig. 2B) which increased 30.5-fold in T-5cl6 and 25.5-  
275 fold in T-4cl3 between 50 and 550 PPF. Furthermore, at 50, 150, 300 and 550 PPF, there was  
276 respectively 2, 4, 3 and 2.5 more Dtx in T-5cl6 than in T-4cl3. In parallel, the de-epoxidation  
277 state of Ddx to Dtx (DES-DD), expressing the conversion of Ddx into Dtx as a photoprotection  
278 mechanism, was calculated (Fig. 2C). At the lowest irradiance of 50 PPF, the DES-DD was 4%  
279 for T-4cl3 and significantly higher for T-5cl6, 9%. For both strains the DES-DD increased with  
280 increasing growth irradiance, and values were higher for T-5cl6 at all four growth irradiances.  
281 At the highest irradiance, 550 PPF, the DES-DD reached 66% for T-5cl6 and 40% for T-4cl3  
282 (Fig. 2C).

283 The maximum PSII quantum yield ( $F_v/F_m$ ) was expressed as a function of the normalized  
284 amount of Dtx to Chl *a* (Fig. 2D). Trend lines of both strains have a  $R^2 > 0.97$ , which  
285 demonstrated a solid correlation between  $F_v/F_m$  and Dtx (Fig. 5D). The slope of the T-4cl3 trend  
286 line was higher than the one of T-5cl6.

287



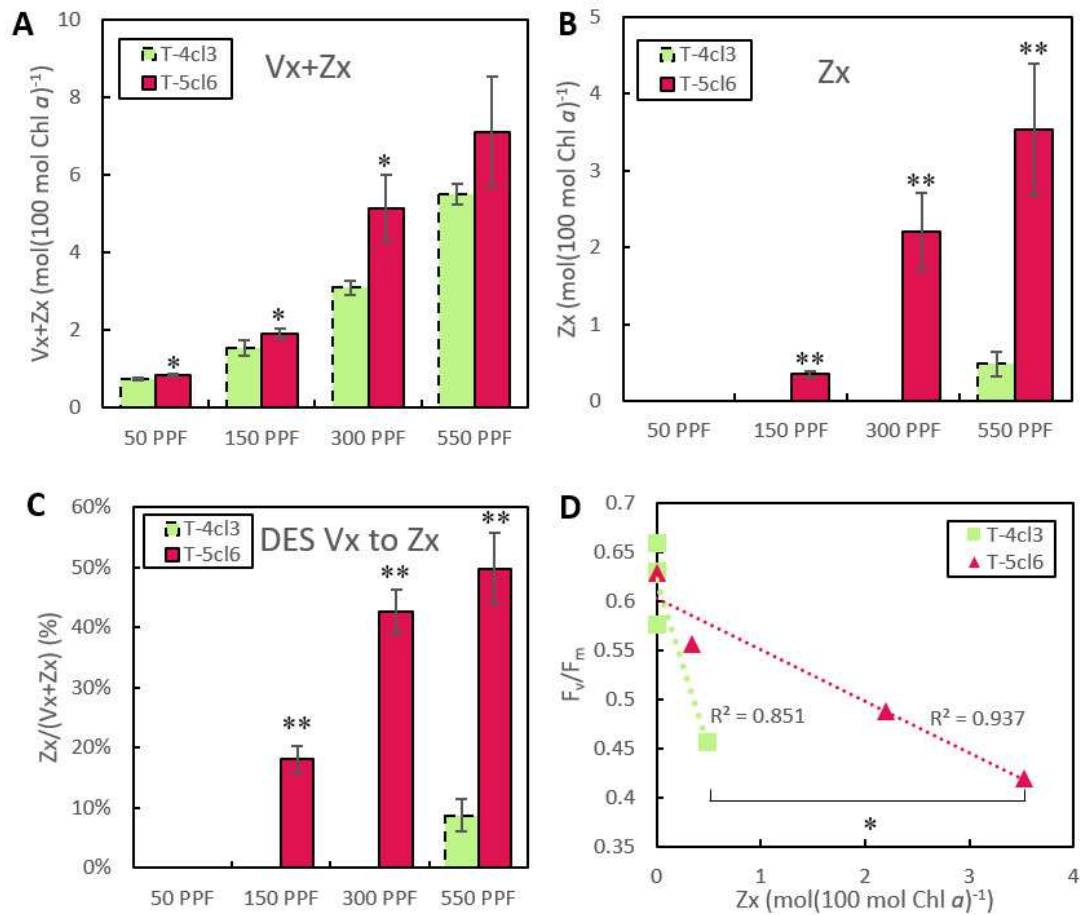
288

289 **Figure 2:** Evolution of the Ddx+Dtx pool (A) and of the Dtx (B) normalized by Chl  $a$  (average  
 290  $\pm$  the confidence interval, mol(100 mol Chl  $a$ )<sup>-1</sup>), of the de-epoxidation state (DES) from Ddx  
 291 into Dtx (C) relatively to growth irradiance (PPF = Photosynthetic Photon Flux =  $\mu\text{mol m}^2 \text{s}^{-1}$ ).  
 292 (D) presents the  $F_v/F_m$  relatively to Dtx content and the significant difference between the two  
 293 slopes. \*: pvalue < 0.05, \*\*: pvalue < 0.01.

294

295 The  $V_x+Z_x$  pool size increased with increasing growth irradiance, and values for T-5cl6 were  
 296 significantly higher than for T-4cl3 (Fig. 3A). As for Dtx,  $Z_x$  was significantly higher in T-5cl6  
 297 from 150 to 550 PPF than in T-4cl3 where  $Z_x$  was synthesized in small amounts at 550 PPF  
 298 only (Fig. 3B). Values of the de-epoxidation state from  $V_x$  to  $Z_x$  (DES-VZ) showed that in T-  
 299 5cl6,  $V_x$  was converted into  $Z_x$  gradually with increasing growth irradiance, and reached 50%  
 300 at 550 PPF (Fig. 3C). In T-4cl3, only 9% of  $V_x$  was converted into  $Z_x$  at 550 PPF.  $F_v/F_m$  was  
 301 expressed relatively to the photoprotective pigment  $Z_x$  (Fig. 3D). The slope of T-4cl3 was  
 302 higher than the one of T-5cl6, it was associated with 6.5-fold less  $Z_x$  than in T-5cl6.

303



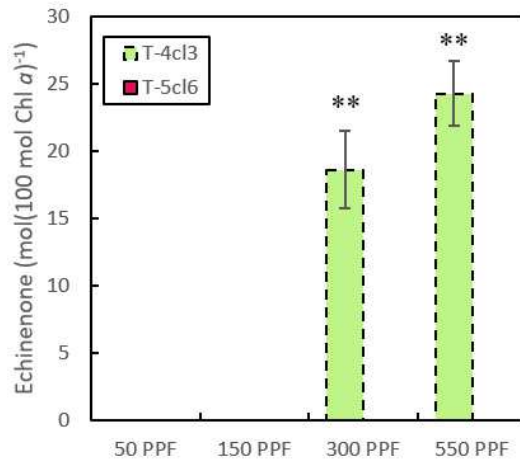
304  
305

306 **Figure 3:** Evolution of the Vx+Zx pool (A) and of the Zx (B) normalized by Chl *a* (average ±  
307 the confidence interval, mol(100 mol Chl *a*)<sup>-1</sup>), of the de-epoxidation state from Vx into Zx (C)  
308 relatively to growth irradiance (PPF = Photosynthetic Photon Flux = μmol m<sup>2</sup> s<sup>-1</sup>). (D) presents  
309 the F<sub>v</sub>/F<sub>m</sub> relatively to Zx content and the significant difference between the two slopes. \*:  
310 pvalue < 0.05, \*\*: pvalue < 0.01.

311

312 In our growth conditions, the pigment echinenone was found only in T-4cl3 strain at 300 PPF  
313 and 550 PPF, and was increasing with growth irradiance (Fig. 4). At 550 PPF, echinenone  
314 represents 17% of the total carotenoids in T-4cl3 and 24% of the Chl *a* amount.

315



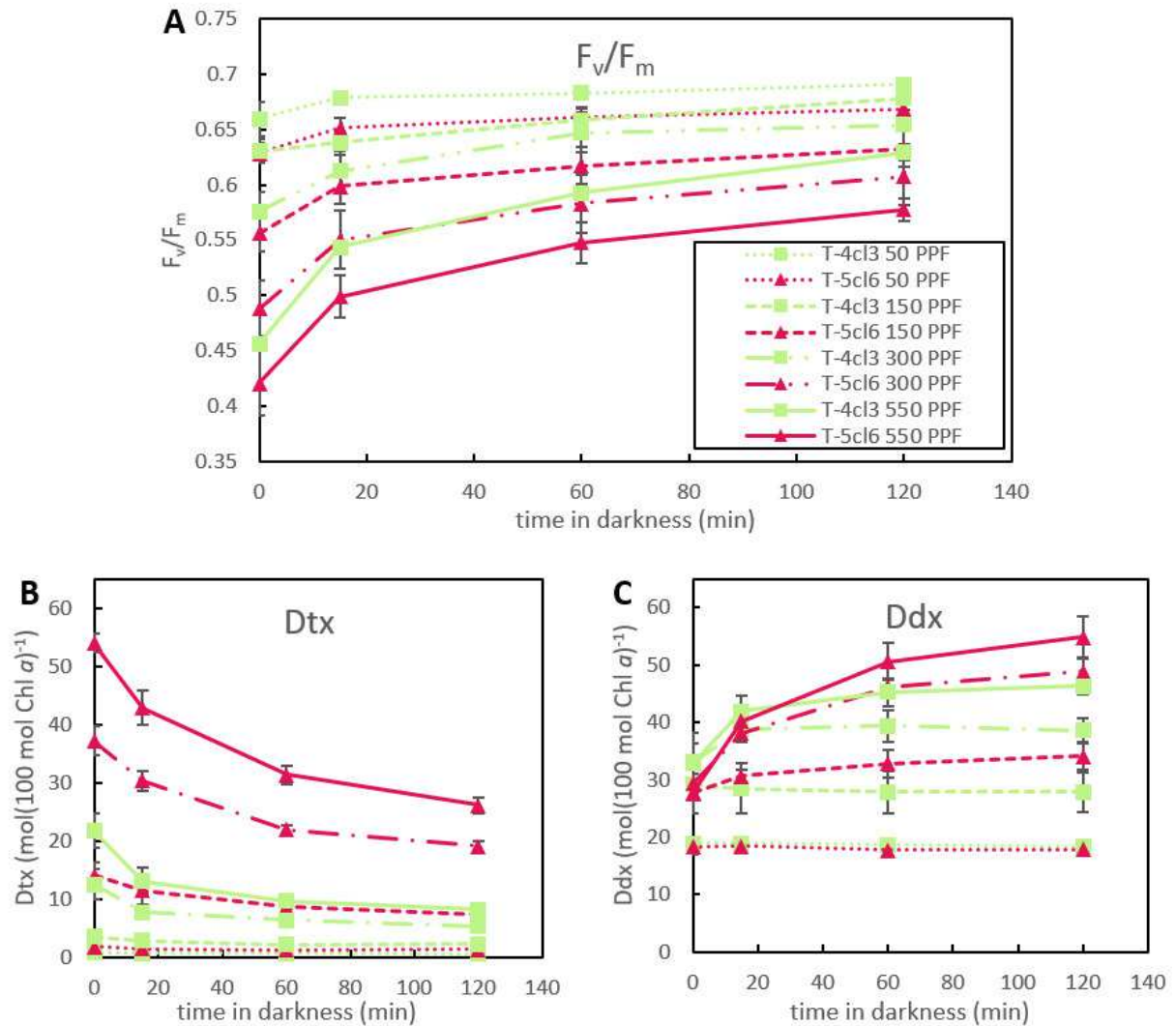
316

317 **Figure 4:** Evolution of the echinenone normalized by Chl *a* (average  $\pm$  the confidence interval,  
 318 mol(100 mol Chl *a*)<sup>-1</sup>) relatively to growth irradiance (PPF = Photosynthetic Photon Flux =  
 319  $\mu\text{mol m}^2 \text{s}^{-1}$ ). \*\*: pvalue < 0.01.

320

321 In order to observe the dynamic balance between photosynthesis and photoprotection, we  
 322 measured the  $F_v/F_m$  and the pigment content of cultures after 0 min, 15 min, 1 hour and 2 hours  
 323 of darkness for each growth irradiance (Fig. 5A). For all conditions,  $F_v/F_m$  was lower in T-5cl6  
 324 than in T-4cl3. For all growth irradiances,  $F_v/F_m$  strongly increased after 20 min of darkness  
 325 and kept increasing after 60 and 120 min. In parallel, Dtx content gradually decreased while  
 326 Ddx content gradually increased as Dtx was re-epoxidized into Ddx (Fig. 5B, 5C). Both  
 327 pigments were higher in T-5cl6 than in T-4cl3. At 550 and 300 PPF, Ddx and Dtx contents  
 328 respectively doubled and halved after 120 min of darkness in T-5cl6. Proportions were lower  
 329 in T-4cl3. After 120 min of darkness, there was still Dtx left in the culture samples of both  
 330 strains which increased with growth irradiance.

331



332

333 **Figure 5:** Evolution of  $F_v/F_m$  (A), of Dtx content (B) and of Ddx content (C) normalized by Chl  
 334  $a$  (average  $\pm$  the confidence interval, mol(100 mol Chl  $a$ )<sup>-1</sup>) relatively to the time in darkness.

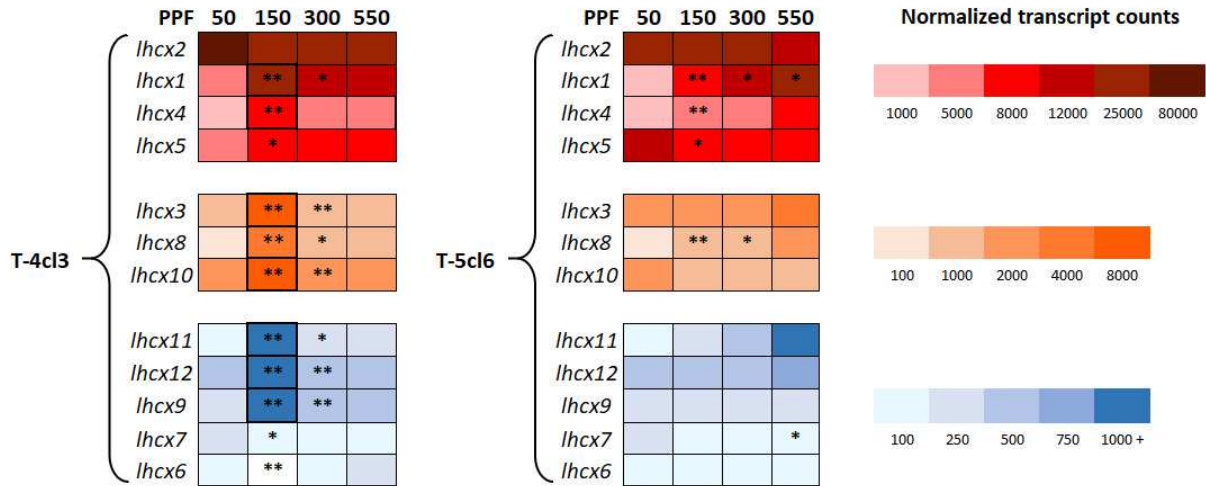
335

### 336 3.3. Expression of *lhc* genes

337 We observed the evolution of the *lhc*x expression in both strains under the four growth  
 338 irradiances (Fig. 6, Fig. S1). The heatmap in Fig. 6 shows the expression level of *lhc*x genes  
 339 and the significant difference between the four growth irradiances for both strains. Transcripts  
 340 amounts of *lhc*x2 were by far the highest especially at 50 PPF in T-4cl3, followed by *lhc*x1  
 341 transcripts accounts. In T-4cl3, 8 *lhc*x upon 12 were remarkably and significantly upregulated  
 342 at 150 PPF (*lhc*x1, *lhc*x3, *lhc*x4, *lhc*x8, *lhc*x9, *lhc*x10, *lhc*x11, *lhc*x12).

343





344

345 **Figure 6:** Heatmap of the *lhcx* transcripts counts. \*: pvalue < 0.05, \*\*: pvalue < 0.01. Thick  
 346 borders correspond to the highly upregulated *lhcx* genes at 150 PPF in T-4cl3.

347

348 Overlooking the upregulation at 150 PPF, *lhcx1*, *lhcx3*, *lhcx4*, *lhcx8* and *lhcx11* were gradually  
 349 upregulated with increasing growth irradiance in both strains, up to five to ten-fold. At the  
 350 highest growth irradiance (550 PPF), these genes were more expressed in T-5cl6 than in T-4cl3.  
 351 In T-4cl3, *lhcx2* and *lhcx7* were upregulated at 50 PPF and *lhcx5* was downregulated at 50 PPF.  
 352 On the contrary, *lhcx2*, *lhcx5* and *lhcx7* were gradually downregulated with increasing growth  
 353 irradiance in T-5cl6.

354

355 In T-4cl3 among the 12 *lhcr*, 10 were downregulated from 150 PPF to 550 PPF (Fig. S2), their  
 356 expression was minimum at 50 PPF (Fig. S2). In T-5cl6, a similar pattern was observed, 10  
 357 *lhcr* were downregulated with increasing growth irradiance from 50 to 550 PPF (all but *lhcr5*  
 358 and *lhcr6*) (Fig. S2). In T-4cl3, *lhcr5* and *lhcr6* were upregulated only under 150 PPF (Fig. S2),  
 359 like the majority of *lhcx* (Fig. 6), while in T-5cl6 they were upregulated with increasing growth  
 360 irradiance. None of the *lhcf* genes were remarkably upregulated at 150 PPF (Fig. S3). In T-4cl3,  
 361 the decreasing pattern with increasing growth irradiance from 50 to 550 PPF was only obvious  
 362 for *lhcf13*, *lhcf21*, *lhcf24*, *lhcf26* and *lhcf27*. In T-5cl6, all 28 *lhcf* were downregulated with  
 363 increasing growth irradiance (Fig. S3). The expression of other genes in T-4cl3 was either  
 364 relatively stable without significant variations, either slightly decreased from 150 PPF to 300  
 365 and 550 PPF. Indeed, in T-4cl3, 15 *lhcf* among 28 were the least expressed at 50 PPF compared  
 366 with other irradiances (*lhcf1*, *lhcf2*, *lhcf3*, *lhcf4*, *lhcf5*, *lhcf6*, *lhcf7*, *lhcf8*, *lhcf17*, *lhcf18*, *lhcf19*,  
 367 *lhcf20*, *lhcf22*, *lhcf25*, *lhcf28*). At 50 PPF, except for *lhcf22* and *lhcf23*, all *lhcf* were more

368 expressed in T-5cl6 than in T-4cl3. Under the other growth irradiances, almost half of *lhcf* (12  
369 among 28) were more expressed in T-5cl6 than in T-4cl3.

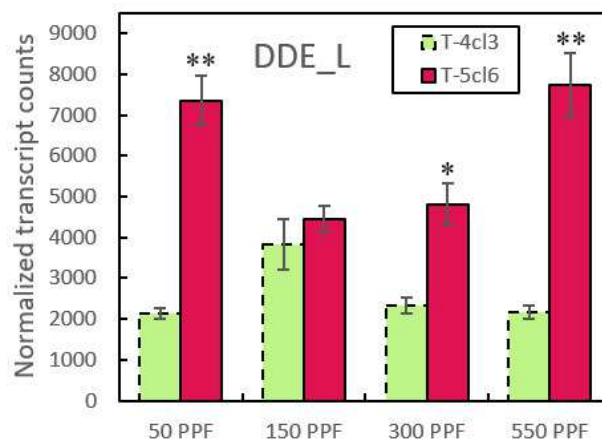
370

### 371 **3.4. Expression of de-epoxidase and epoxidase genes**

#### 372 **3.4.1. Diadinoxanthin de-epoxidase, DDE**

373 The similarity research with the DDE of *T. pseudonana* as a query resulted in four *T. lutea*  
374 genes, with the best similarity score for TISO\_37047 (259) (Table S1). Furthermore,  
375 TISO\_37047 had lower similarity scores with all other VDE, VDL (violaxanthin de-epoxidase  
376 like) or VDR (violaxanthin de-epoxidase related) of diatoms than with the DDE of *T.*  
377 *pseudonana*, although it had higher scores with a VDE domain-containing protein of the  
378 haptophyte *E. huxleyi*. Considering the fact that no DDE was annotated yet for haptophytes,  
379 and that VDE and DDE domains might resemble, TISO\_37047 was the best candidate as a  
380 putative DDE enzyme. We decided to annotate this gene as DDE\_L (DDE\_like) in *T. lutea*.  
381 According to the Interproscan analysis of this sequence, DDE\_L possesses several VDE  
382 domains (Table S5). We noticed that in all Interproscan database, there was no DDE domain  
383 referenced. We monitored the evolution of DDE\_L expression as a function of growth  
384 irradiance (Fig. 7). DDE\_L expression in T-5cl6 was higher than in T-4cl3 under all four growth  
385 irradiances, and significantly at 50, 300 and 550 PPF. At 50 and 550 PPF, DDE\_L was 3.5  
386 times more expressed in T-5cl6 (p-value < 0.01), and transcripts accounts at these two  
387 irradiances were similar in both strains respectively. More generally, in T-5cl6, DDE\_L  
388 expression increased gradually from 150 to 550 PPF while in T-4cl3 transcripts accounts were  
389 similar at 50, 300 and 550 PPF and maximum at 150 PPF (Fig. 7). No Dtx-epoxidase were  
390 found in the UniprotKB database.

391



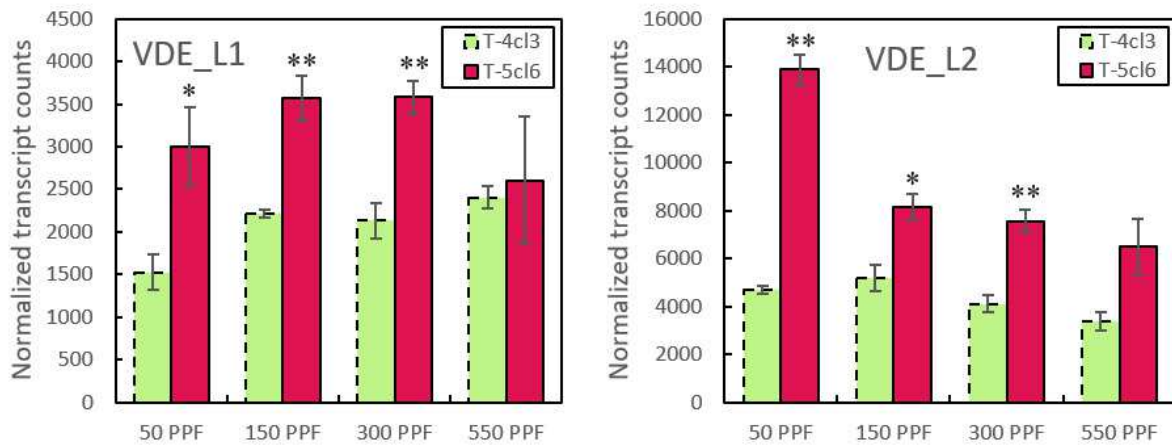
392

393 **Figure 7:** Evolution of normalized transcript counts of DDE\_L (average  $\pm$  the confidence  
 394 interval) relatively to growth irradiance (PPF = Photosynthetic Photon Flux =  $\mu\text{mol m}^2 \text{s}^{-1}$ ). \*:   
 395 pvalue < 0.05, \*\*: pvalue < 0.01.

396

397 3.4.2. *Violaxanthin de-epoxidase, VDE and zeaxanthin epoxidase, ZE*

398



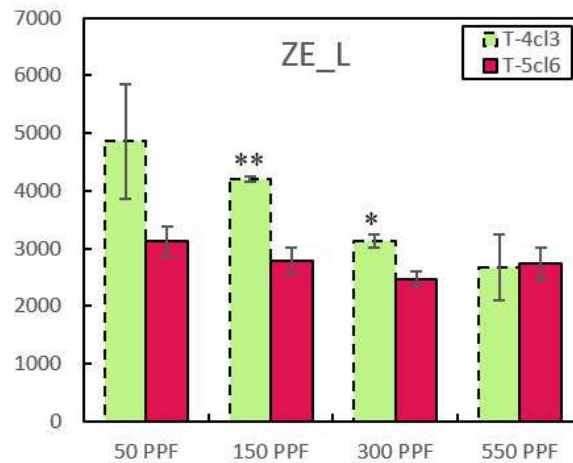
399

400 **Figure 8:** Evolution of TISO\_01606 (VDE\_L1) and TISO\_02731 (VDE\_L2) normalized  
 401 transcripts counts (average  $\pm$  the confidence interval) relatively to growth irradiance (PPF =  
 402 Photosynthetic Photon Flux =  $\mu\text{mol m}^2 \text{s}^{-1}$ ). \*: pvalue < 0.05, \*\*: pvalue < 0.01.

403

404 The similarity research with the VDE, VDL and VDR of diatoms and haptophytes as a query  
 405 resulted in five *T. lutea* genes. The same five genes were found throughout the similarity  
 406 research with diatoms and the one with haptophytes. According to Interproscan analysis of the  
 407 molecular function, all five genes possess a VDE activity (Table S5). The best similarity scores  
 408 were obtained with haptophyte sequences. TISO\_01606 especially obtained the highest  
 409 similarity score of all sequences, with the VDE2 sequence of *E. huxleyi* (600, Table S2).  
 410 TISO\_01606 was named VDE\_L1 (VDE\_Like1) and considered as coding for a putative VDE  
 411 enzyme. The alignment of VDE\_L1 of *T. lutea* and VDE2 of *E. huxleyi* resulted in 67.4%  
 412 similarity. Interestingly, VDE\_L1 expression was significantly higher in T-5cl6 than in T-4cl3  
 413 at 50, 150 and 300 PPF but not at 550 PPF (Fig. 8). In T-5cl6, VDE\_L1 increased from 50 to  
 414 150 PPF then stabilized at 300 PPF and decreased at 550 PPF. TISO\_02731 showed high  
 415 similarity score with the VDE of *C. tobinii* and a VDE domain-containing protein of *E. huxleyi*  
 416 (respectively 418 and 400) (Table S2), and as such was considered as coding for a putative  
 417 VDE enzyme. TISO\_02731 was named VDE\_L2 (for VDE\_Like2). VDE\_L2 expression was  
 418 higher in T-5cl6 than in T-4cl3 under all growth irradiances, and significantly at 50, 150 and

419 300 PPF (Fig. 8). In both strains, but especially in T-5cl6, its expression decreased with  
 420 increasing irradiance. According to Interproscan analysis (Table S5), VDE\_L2 was associated  
 421 with two biological processes, potassium ion transport and transmembrane transport, and two  
 422 molecular functions, voltage-gated potassium channel activity and VDE activity. VDE\_L2 was  
 423 the only gene which was not exclusively associated to VDE activity among the five genes found  
 424 with the similarity research.  
 425



426  
 427 **Figure 9:** Evolution of TISO\_33049 (ZE\_L) normalized transcripts counts (average  $\pm$  the  
 428 confidence interval) relative to growth irradiance (PPF = Photosynthetic Photon Flux =  $\mu\text{mol}$   
 429  $\text{m}^2 \text{s}^{-1}$ ). \*: pvalue < 0.05, \*\*: pvalue < 0.01.

430  
 431 The similarity research with the ZE of diatoms and haptophytes as a query resulted in eleven *T.*  
 432 *lutea* genes (Table S3, S4). Among them, TISO\_30349 had the highest similarity score with a  
 433 ZE in *E. huxleyi* (578) (Table S4). TISO\_30349 was therefore considered as coding for a  
 434 putative ZE enzyme and named ZE\_L (for ZE\_Like). With increasing growth irradiance, the  
 435 expression of ZE\_L decreased in both strains (Fig. 9). At 150 and 300 PPF, ZE\_L was  
 436 significantly more expressed in T-4cl3.

## 437 438 **4. Discussion**

### 439 **4.1. Different photoprotection strategies in *T. lutea* T-5cl6 and T-4cl3 strains**

#### 440 **4.1.1. The Ddx-Dtx and Vx-Zx xanthophyll cycles**

441 As cells maintained growth efficiency under light stress, as shown with the increasing growth  
 442 rate in Fig. S4, the observed molecular events such as photoprotective pigments synthesis really  
 443 protected the cells from damage. The two *T. lutea* clonal strains, T-5cl6 and T-4cl3, were grown  
 444 in the exact same conditions of irradiance, temperature, pH, nutrients, and at the same cell

445 concentration. The ratio of Fx/Chl *a* was lower in T-4cl3 than in T-5cl6, suggesting that the  
446 light-harvesting capacity under high light was lower in T-4cl3. Using the darkness relaxation  
447 of F<sub>v</sub>/F<sub>m</sub> as a proxy for NPQ [29], we monitored a strong correlation with the Dtx content,  
448 pointing out to an implication of Dtx in the photoprotective dissipation of excess light energy  
449 in both strains. The decrease of photochemistry in T-4cl3 was associated to 2.5-fold less amount  
450 of Dtx than in T-5cl6, suggesting differences in quenching efficiency of Dtx between the two  
451 strains. Moreover, as in diatoms, Ddx was not entirely de-epoxidized in Dtx (*i.e.* maximum  
452 DES was about 60%), highlighting the double role of Ddx as a photosynthetic pigment and as  
453 a precursor of Dtx [35]. The same hold true for the photoprotective couple pigment Vx and Zx,  
454 as previously reported in diatoms [36]. In T-5cl6, photoprotection was associated with a higher  
455 Dtx and Zx content than in T-4cl3, with Zx only accumulated at 550 PPF in T-4cl3. Instead, T-  
456 4cl3 produced echinenone at 300 and 550 PPF while T-5cl6 did not. In summary, T-5cl6 used  
457 the two xanthophyll cycles Ddx-Dtx and Vx-Zx, and associated NPQ, as major photoprotective  
458 mechanisms, similarly as in diatoms [16]. Both cycles were used to a lower extent and more  
459 sequentially by T-4cl3. In addition, T-4cl3 cells strengthened their photoprotective pigment  
460 panel by producing echinenone at a certain threshold between 150 and 300 PPF. At 550 PPF,  
461 Dtx and echinenone were probably not sufficient to endorse the excess light energy in T-4cl3  
462 cells and they started de-epoxidizing Vx into Zx. It is likely that at higher irradiances above  
463 550 PPF, the Zx and echinenone concentrations would increase even more.

464

#### 465 4.1.2. *The remarkable presence of echinenone in T-4cl3*

466 The most noteworthy result of this study was the appearance of echinenone in T-4cl3 cells at  
467 300 PPF. The presence of echinenone was previously demonstrated in *T. lutea* strain CCAP  
468 927/14 [37] and in a close species, *Isochrysis galbana*, under N-deprivation [37,38]. In addition,  
469 we observed that T-4cl3 also synthesized echinenone under N-deprivation (Pajot *et al.* in prep).  
470 In *T. lutea* strain CCAP 927/14, it was reported that echinenone represented 25% of total  
471 carotenoids under N-deprivation [37]. Our results showed that echinenone represented a similar  
472 high amount of 17% of total carotenoids under N-replete condition at high irradiance.  
473 Echinenone is usually found in cyanobacteria, it scavenges the ROS [39] under high irradiance,  
474 and as such participates to photoprotection. In cyanobacteria, under high irradiance, the thermal  
475 dissipation of the light energy absorbed in excess by the phycobilisome (the light-harvesting  
476 antenna of cyanobacteria) is also mediated by a NPQ mechanism, which regulatory partners are  
477 different from haptophytes and diatoms [40]. Cyanobacteria NPQ occurs when the echinenone  
478 is bound to the Orange Carotenoid Protein (OCP) [41,42]. For instance, in *Synechocystis sp.*,

479 NPQ is only activated when the 3'-hydroxyechinenone is bound to the OCP [43]. Our work is  
480 a first report of the presence of echinenone in a haptophyte under high light. According to  
481 several similarity researches we performed, no OCP was found in *T. lutea*. However, our results  
482 support that in the strain T-4cl3, the echinenone played a role in the response to high light as a  
483 support to the xanthophyll cycles-mediated NPQ, likely through direct ROS scavenging [44],  
484 *i.e.* by free-echinenone molecules in the thylakoid membrane, similarly as some Dtx molecules  
485 [45]. Nevertheless, we cannot exclude that a different form of the OCP is present in *T. lutea*,  
486 and further search is required.

487

#### 488 **4.2. Xanthophyll de-epoxidases and epoxidases in *T. lutea***

489 This is the first time that several DDE and VDE candidate genes were characterized in *T. lutea*.  
490 The monitoring of their expression as a function of growth irradiance enabled to correlate the  
491 transcription of these genes to the different light-response strategies shown by T-5cl6 and T-  
492 4cl3. No Dtx-epoxidase was found in the UniprotKB database. However, the two Dtx-  
493 epoxidases of *Thalassiosira pseudonana* are usually annotated as ZE in the literature [46].  
494 Therefore, the seven sequences in *T. lutea* resulting from the research similarity with the query  
495 sequence “ZE *Thalassiosira pseudonana* THAPSDRAFT 261390” (Table S3) might be good  
496 candidates as Dtx-epoxidase.

497

498 As pointed out before in the diatom *P. tricornutum*, the zeaxanthin-epoxidase (ZE) can play an  
499 equivalent role, *i.e.* ZE can trigger the epoxidation of both Dtx and Zx [30,43].

500

##### 501 **4.2.1. The diadinoxanthin de-epoxidase**

502 With increasing growth irradiance, Ddx was de-epoxidized into Dtx as illustrated by the  
503 progressive increase in DES-DD in both strains. Ddx de-epoxidation was stronger in T-5cl6  
504 than in T-4cl3. We found a DDE gene candidate we named DDE\_L, whose associated protein  
505 could be responsible of the Ddx de-epoxidation in *T. lutea*. As for Dtx content and DES-DD,  
506 DDE\_L expression was higher in T-5cl6 than in T-4cl3 under all four irradiances, which was  
507 consistent with a stronger Ddx de-epoxidation activity in T-5cl6. Interestingly, in T-5cl6, the  
508 expression of DDE\_L was close to its maximum already at 50 PPF. In parallel, we did not  
509 observe a particular Dtx accumulation that could have been induced by chlororespiratory  
510 electron flow, as it was reported in the diatom *Phaeodactylum tricornutum* [48]. This result  
511 might suggest that T-5cl6 cells produce a maximum of DDE\_L transcripts regardless of the  
512 irradiance, without translating them into protein unless it is necessary. Or, the associated protein

513 of DDE\_L has a more complex role than the putative de-epoxidation of Ddx. In *P. tricornutum*,  
514 the inactivation of the DDE enzyme under low light was shown not to be the factor triggering  
515 the inactivation of Dtx synthesis and NPQ maintenance [47]. Instead, they were due to an  
516 increase in Dtx epoxidation, which was therefore proposed to be the main actor in the Ddx-Dtx  
517 xanthophyll cycle regulation.

518

#### 519 4.2.2. *The violaxanthin de-epoxidase and the zeaxanthin epoxidase*

520 The difference between the two clonal strains was also witnessed by the expression level of the  
521 Vx-Zx cycle associated genes. Among them, the expression of TISO\_01606, we named  
522 VDE\_L1, was significantly higher in T-5cl6 at almost all growth irradiances, and it increased  
523 with increasing growth irradiance. A second putative candidate, TISO\_02731, we named  
524 VDE\_L2, was found to be associated to both a VDE activity and a voltage-gated potassium  
525 channel protein. A voltage-gated potassium channel protein is a complex forming a  
526 transmembrane channel through which potassium ions may cross a cell membrane in response  
527 to changes in membrane potential [49]. It is noteworthy that VDE\_L2 could regulate in parallel  
528 both the de-epoxidation of Vx and the pH lumen which is itself pH-dependent [20,50]. Such  
529 potential dual role would need further investigation, ideally with targeted knock-out  
530 mutagenesis, as in diatoms [51]. Furthermore, VDE\_L1 in *T. lutea* had the best similarity score  
531 with the VDL2 gene of *P. tricornutum* (gene identification: PHATRDRAFT\_45846), which  
532 encodes for an enzyme that has recently been demonstrated to be central in the Fx biosynthetic  
533 pathway in a study by Bai *et al.* (2022) [52]. This study suggested that Ddx would also be a  
534 substrate for the VDL2 enzyme, in addition to Vx. VDL2 would indeed be able to catalyze the  
535 tautomerization reaction (isomerization of a molecular function) of Ddx to allenoxanthin, these  
536 two pigments being key precursors of the Fx synthesis [52]. In addition, it is specified that the  
537 VDL2 enzyme in *P. tricornutum* is most likely subject to strict regulation in diatoms and  
538 haptophytes, so that Ddx can play both its role as a precursor of the major photosynthetic  
539 pigment that is Fx, and its role in photoprotection within the Ddx-Dtx cycle.

540

541 In the diatom *P. tricornutum*, NPQ results from the early inhibition of ZE rather than from an  
542 activation of DDE/VDE, which increases the amount of Dtx and, under certain light conditions,  
543 of Zx [47]. The epoxidation is the reverse reaction of the Ddx-Dtx and Vx-Zx cycles and it  
544 usually corresponds to a decrease in light intensity. In *T. lutea*, ZE\_L gene seems to be a strong  
545 candidate to code for a zeaxanthin epoxidase. In both strains, the ZE-L transcript level was  
546 similar to the ones of DDE and VDE, it was the highest at 50PPF, and its expression decreased

547 with increasing growth irradiance, and might correspond to a lower synthesis of the ZE\_L  
548 associated protein. This pattern is usual and might be interpreted as the need of cells for keeping  
549 the right balance between light-harvesting (Ddx and Vx) and photoprotective (Dtx and Zx)  
550 pigments as a function of the growth irradiance. In the study by Bai *et al.*, (2022) [52], the ZEP1  
551 (zeaxanthin epoxidase) gene in *P. tricornutum* (gene identification: PHATR DRAFT\_45845)  
552 has been shown, as VDL2, to code for a central enzyme in the Fx biosynthetic pathway [52].  
553 Since ZE\_L in *T. lutea* had a high similarity score with ZEP1, it is assumed that its role, in  
554 addition to the epoxidation of Zx, is also central in the biosynthesis of Fx in *T. lutea* and in  
555 haptophytes in general.

556

### 557 **4.3. A sustained NPQ in *T. lutea***

558 Culture samples were exposed to darkness in order to observe the relaxation dynamics from  
559 photoprotection back to photochemistry. Surprisingly, after two hours of darkness exposure,  
560 there was still Dtx present in cells of both strains, indicating that the epoxidation reaction from  
561 Dtx to Ddx was not complete. It has been determined that in algae using the Ddx-Dtx cycle as  
562 a photoprotective mechanism, the switch of the light-harvesting antenna from the NPQ mode  
563 to the light-harvesting mode at lower irradiance can only be realized by an efficient removal of  
564 Dtx [53]. Nevertheless, under some harsh conditions (very high light, low temperature), the  
565 presence of Dtx, even after prolonged darkness, *i.e.* several hours and days, can be ‘constitutive’  
566 and can generate a sustained form of NPQ [28,29]. This form of NPQ is complementary to the  
567 main NPQ component, qE [28,46,54], which is usually turned off in a few tens of seconds to  
568 some minutes when the cells are transferred from excess light to lower light or darkness [10].  
569 In *T. lutea*, the retention of Dtx under prolonged darkness was especially strong in T-5cl6 under  
570 the highest irradiances. It was correlated with a partial relaxation on  $F_v/F_m$  likely illustrating a  
571 strong sustained NPQ [29]. It is noteworthy that T-5cl6 is the strain which relies the most on  
572 xanthophyll cycles. A stronger sustained NPQ is likely to be part of its photoprotective strategy,  
573 allowing the cells to promptly respond to an anticipated increase in irradiance after the darkness  
574 period [29].

575

### 576 **4.4. The role of *lhcx* in *T. lutea***

#### 577 **4.4.1. *lhcx1*, *lhcx4*, *lhcx8* and *lhcx11* as major actors in regulating NPQ?**

578 The increase of photoprotective pigments such as Dtx and Zx does not necessarily lead to higher  
579 effective NPQ. Indeed in diatoms, it is the binding of photoprotective pigments to Lhc proteins,  
580 especially Lhc, that effectively involves these pigments in NPQ [10]. Dtx molecules can be



581 freely present in the thylakoid membrane to directly scavenge ROS species [45]. In both *T.*  
582 *lutea* strains, *lhcx1*, *lhcx4*, *lhcx8* and *lhcx11* were gradually upregulated with increasing growth  
583 irradiance together with Dtx synthesis. It suggests that *lhcx1*, *lhcx4*, *lhcx8* and *lhcx11* could be  
584 Dtx binders and potentially major actors in regulating NPQ in *T. lutea*. Interestingly, the  
585 transcript level of these genes was not particularly different between both strains (but for 150  
586 PPF, see below) although NPQ was significantly stronger in T-5cl6, with the only exception of  
587 *lhcx11* at 550 PPF for which there was no difference in NPQ. Therefore, the NPQ difference  
588 can only be explained by the highest transcription of *lhcx* genes in corresponding proteins in T-  
589 5cl6 for providing the necessary binding sites to the significantly higher amount of Dtx  
590 molecules in this strain. Western-blot analysis will be needed to further confirm this hypothesis  
591 [17,55]. Besides *lhcx*, two *lhcr* genes, *lhcr5* and *lhcr6*, were upregulated with increasing growth  
592 irradiance in both strains. Interestingly, *lhcr5* and *lhcr6* form, together with *lhcr10*, a subclade  
593 of the *lhcr* family in *T. lutea* [15]. Moreover, *lhcr5* and *lhcr6* are similar to *lhcr6* and *lhcr8* in  
594 *P. tricornutum*, which were proposed to play a role in photoprotection [15,56]. It is therefore  
595 consistent that *lhcr5* and *lhcr6* were expressed similarly to the majority of *lhcx* in T-4cl3. This  
596 result confirmed their supposed function in photoprotection, and possibly in NPQ.

597

#### 598 4.4.2. *lhcx2* and *lhcx5* prevent an increase in irradiance?

599 Among *lhcx* genes, *lhcx2*, *lhcx5* and *lhcx7* were the only genes downregulated with increasing  
600 growth irradiance. In particular, *lhcx2* was highly expressed at 50 PPF in T-4cl3. Similarly, in  
601 our previous study on *T. lutea* strain CCAP 927/14, *lhcx2* was the only gene upregulated at low  
602 light, and during the night [15]. The hypothesis was that the associated Lhcx2 protein could  
603 protect from the return of light at any time after prolonged darkness exposure, as proposed for  
604 Lhcx4 in the diatom *P. tricornutum* [57]. The function of *lhcx2* in *T. lutea* strain CCAP 927/14  
605 and T-4cl3 might therefore be extended to respond to a potential increase of irradiance during  
606 a low light period acclimation. In T-5cl6, this role might be undertaken by *lhcx5* which was  
607 also highly expressed at 50 PPF compared with T-4cl3. Transcript accounts of *lhcx2* and *lhcx5*,  
608 as well as the high light upregulated *lhcx1* and *lhcx4*, were the highest in both strains. Thus,  
609 corresponding proteins, if translation would be paralleled, might play an important role in light-  
610 response and possibly be predominant in the structure of the FCP in *T. lutea*.

611

#### 612 4.4.3. *lhcx* participate in the balance between photochemistry and photoprotection?

613 We observed a significant spike of expression for eight *lhcx* and two *lhcr* (*lhcr5* and *lhcr6*) at  
614 150 PPF in T-4cl3. It was not paralleled with photoprotective pigments. The increase of *lhcx*

615 and *lhcr* expression at 150 PPF was therefore not considered as inherent to photoprotection  
616 mechanisms under to the highest irradiances. In a previous experiment, the same 8 *lhcx* of *T.*  
617 *lutea* strain CCAP 927/14, cultivated with a day:night cycle, were significantly upregulated at  
618 the beginning of the day, corresponding to 225 PPF, compared to midday, corresponding to 900  
619 PPF [15]. The hypothesis was that cells overexpressed *lhcx* at the beginning of the day to  
620 endorse light onset without risking photodamage. With our results in this work, the explanation  
621 could finally be different. We hypothesize that 150 PPF is a threshold between photochemistry  
622 and photoprotection for T-4cl3, *i.e.* that 150 PPF would be close to  $E_K$ , the light saturation  
623 parameter for growth. This possibility is supported by the sharper decrease in  $F_v/F_m$  beyond 150  
624 PPF in T-4cl3. Another possibly, not exclusive, and depending on transcript translation, is the  
625 need for specific *Lhcx* and/or *Lhcr* FCP subunits in the light-harvesting antenna, in order to  
626 perform the best adjustment between photochemistry and photoprotection at 150 PPF and  
627 beyond.

628

## 629 **5. Conclusion**

630 This study investigated the differences of photoprotection strategies between two clonal strains  
631 of the haptophyte *Tisochrysis lutea*. Overall, our results showed that with increasing growth  
632 irradiance, the expression of the *lhcx* genes increased and it was correlated with a gradual  
633 increase of the content in photoprotective pigments and of the dissipation of light energy in  
634 excess. Both strains differed with their photoprotective pigment (Table 2). T-5cl6 strain strategy  
635 was predominantly based on the Ddx-Dtx and the Vx-Zx xanthophyll cycles, while T-4cl3  
636 strain strategy was also based on the Ddx-Dtx cycle, but to a lesser extent, and on the parallel  
637 echinenone accumulation. At higher irradiances, when both Dtx and echinenone appeared to be  
638 insufficient to endorse the excess light energy, the photoprotective pigment content was  
639 completed with the Vx-Zx cycle.

640

641 In both strains, the fine balance between photosynthesis and photoprotection was performed by  
642 the combination of (Table 2) (1) the FCP structuration with *lhcx*, *lhcr* and *lhcf*, (2) the  
643 modulation of the photosynthetic pigments chlorophylls and fucoxanthin, (3) the synthesis of  
644 photoprotective pigments of the Ddx-Dtx and the Vx-Zx xanthophyll cycles, alongside with the  
645 transcription of de-epoxidases and epoxidases, and of the echinenone in T-4cl3 specifically.  
646 The differences between the two clonal strains highlighted precise correlations between these  
647 regulatory partners. We propose these differences are likely due to their adaptation to the light  
648 climate of the natural environment from where they were isolated [58–60], and/or to the

649 individual evolution and selection in the laboratory growing conditions. Finally, the remarkable  
650 presence of echinenone, which content was modulated by light under N-replete condition,  
651 excludes the influence of nutrients alone on its biosynthesis.  
652

653 **Table 2:** Summary of the pigment content,  $F_v/F_m$ , *lhcx* and *lhcr* gene expression in T-5cl6 and T-4cl3 cells under the four growth irradiances.

654 Legend for levels: +++ (highest), ++ (high), + (moderately high), - (moderately low), -- (low), 0 (absence).

		Photophysiology	Pigments					<i>lhcx</i> gene expression		
Strain	Light		Dissipation of the light energy in excess	Photosynthetic pigments		Photoprotective pigments			Actors of NPQ	
		Fx		Chl <i>a</i>	Dtx	Zx	Echinenone	<i>lhcx1, lhcx4, lhcx8, lhcx11, lhcr5, lhcr6</i>	<i>lhcx2</i>	<i>lhcx5</i>
<b>T-5cl6</b>	50 PPF	--	+++	+++	-	0	0	--	+	+++
<b>T-4cl3</b>		0	+++	+++	--	0	0	--	+++	-
<b>T-5cl6</b>	150 PPF	-	++	++	+	+	0	-	+	+
<b>T-4cl3</b>		--	++	++	-	0	0	+++	+	++
<b>T-5cl6</b>	300 PPF	+	++	+	++	++	0	+	-	-
<b>T-4cl3</b>		-	+	+	+	0	+	+	-	+
<b>T-5cl6</b>	550 PPF	++	-	-	+++	+++	0	++	--	-
<b>T-4cl3</b>		++	-	-	++	+	++	++	-	+

655

656

657

658 **Funding:**

659 The authors would like to acknowledge Ifremer and the Region Pays de la Loire (France) for  
660 the PhD grant of Anne Pajot. This work was co-funded by the SMIDAP through the TINAQUA  
661 project.

662

663 **Acknowledgements:**

664 The authors would like to thank Gaël Bougaran, Raymond Kaas, Jean-Baptiste Bérard, for their  
665 help with the turbidostat cultures and the sensors, Elise Robert and Agathe Maupetit, for their  
666 participation in the experiments.

667

668 **Conflicts of Interest:**

669 The authors declare no conflict of interest.

670

671 **Data Availability Statement:**

672 The original contributions presented in the study are publicly available. This data can be found  
673 here: National Center for Biotechnology Information (NCBI) BioProject database under  
674 accession number PRJNA787725.

675

676 **Author contributions:**

677 Conceptualization, A.P., E.N., T.L., J.L.; Methodology, A.P., E.N., G.C.; Formal analysis, A.P.,  
678 G.C.; Investigation, A.P., J.L.; Data curation, A.P., G.C.; Writing-Original Draft preparation,  
679 A.P.; Writing-Review & Editing, J.L., E.N., G.C., T.L.; Visualization, A.P.; Supervision, E.N.,  
680 L.M.; Project Administration, E.N., L.M.

681

682 **6. References**

683

- 684 [1] T. Cavalier-Smith, Chromalveolate diversity and cell megaevolution: interplay of  
685 membranes, genomes and cytoskeleton, in: *Organelles, Genomes and Eukaryote*  
686 *Phylogeny: An Evolutionary Synthesis in the Age of Genomics*, Taylor and Francis, CRC  
687 Press, 2004: pp. 71–103.
- 688 [2] A. Telfer, Singlet Oxygen Production by PSII Under Light Stress: Mechanism, Detection  
689 and the Protective role of  $\beta$ -Carotene, *Plant and Cell Physiology*. 55 (2014) 1216–1223.  
690 <https://doi.org/10.1093/pcp/pcu040>.
- 691 [3] A. Edreva, Generation and scavenging of reactive oxygen species in chloroplasts: a  
692 submolecular approach, *Agriculture, Ecosystems & Environment*. 106 (2005) 119–133.  
693 <https://doi.org/10.1016/j.agee.2004.10.022>.

- 694 [4] K.E. Lohman, The ubiquitous diatom - a brief survey of the present state of knowledge,  
695 American Journal of Science. 258 (1960) 180–191.
- 696 [5] M.D. Guiry, How Many Species of Algae Are There?, Journal of Phycology. 48 (2012)  
697 1057–1063. <https://doi.org/10.1111/j.1529-8817.2012.01222.x>.
- 698 [6] B. Edvardsen, E.S. Egge, D. Vaultot, Diversity and distribution of haptophytes revealed  
699 by environmental sequencing and metabarcoding – a review, Pip. 3 (2016) 77–91.  
700 <https://doi.org/10.1127/pip/2016/0052>.
- 701 [7] C. Büchel, Light harvesting complexes in chlorophyll c-containing algae, Biochimica et  
702 Biophysica Acta (BBA) - Bioenergetics. 1861 (2020) 148027.  
703 <https://doi.org/10.1016/j.bbabi.2019.05.003>.
- 704 [8] A. Beer, K. Gundermann, J. Beckmann, C. Büchel, Subunit Composition and  
705 Pigmentation of Fucoxanthin–Chlorophyll Proteins in Diatoms: Evidence for a Subunit  
706 Involved in Diadinoxanthin and Diatoxanthin Binding, Biochemistry. 45 (2006) 13046–  
707 13053. <https://doi.org/10.1021/bi061249h>.
- 708 [9] S.-H. Zhu, B.R. Green, Photoprotection in the diatom *Thalassiosira pseudonana*: Role of  
709 LI818-like proteins in response to high light stress, Biochimica et Biophysica Acta (BBA)  
710 - Bioenergetics. 1797 (2010) 1449–1457. <https://doi.org/10.1016/j.bbabi.2010.04.003>.
- 711 [10] B. Lepetit, S. Sturm, A. Rogato, A. Gruber, M. Sachse, A. Falciatore, P.G. Kroth, J.  
712 Lavaud, High Light Acclimation in the Secondary Plastids Containing Diatom  
713 *Phaeodactylum tricorutum* is Triggered by the Redox State of the Plastoquinone Pool,  
714 Plant Physiology. 161 (2013) 853–865. <https://doi.org/10.1104/pp.112.207811>.
- 715 [11] W. Wang, L.-J. Yu, C. Xu, T. Tomizaki, S. Zhao, Y. Umena, X. Chen, X. Qin, Y. Xin, M.  
716 Suga, G. Han, T. Kuang, J.-R. Shen, Structural basis for blue-green light harvesting and  
717 energy dissipation in diatoms, Science. 363 (2019).  
718 <https://doi.org/10.1126/science.aav0365>.
- 719 [12] C. Büchel, Light-Harvesting Complexes of Diatoms: Fucoxanthin-Chlorophyll Proteins,  
720 in: A.W.D. Larkum, A.R. Grossman, J.A. Raven (Eds.), Photosynthesis in Algae:  
721 Biochemical and Physiological Mechanisms, Springer International Publishing, Cham,  
722 2020: pp. 441–457. [https://doi.org/10.1007/978-3-030-33397-3\\_16](https://doi.org/10.1007/978-3-030-33397-3_16).
- 723 [13] N.L. Fisher, D.A. Campbell, J. Hughes, U. Kuzhiumparambil, K.H. Halsey, P.J. Ralph,  
724 D.J. Suggett, Divergence of photosynthetic strategies amongst marine diatoms, PLOS  
725 ONE. 15 (2020) e0244252. <https://doi.org/10.1371/journal.pone.0244252>.
- 726 [14] S.C. Lefebvre, G. Harris, R. Webster, N. Leonardos, R.J. Geider, C.A. Raines, B.A. Read,  
727 J.L. Garrido, Characterization and expression analysis of the Lhcf gene family in  
728 *Emiliania huxleyi* (haptophyta) reveals differential responses to light and CO<sub>2</sub>., Journal  
729 of Phycology. 46 (2010) 123–134. <https://doi.org/10.1111/j.1529-8817.2009.00793.x>.
- 730 [15] A. Pajot, J. Lavaud, G. Carrier, M. Garnier, B. Saint-Jean, N. Rabilloud, C. Baroukh, J.-  
731 B. Bérard, O. Bernard, L. Marchal, E. Nicolau, The Fucoxanthin Chlorophyll a/c-Binding  
732 Protein in *Tisochrysis lutea*: Influence of Nitrogen and Light on Fucoxanthin and  
733 Chlorophyll a/c-Binding Protein Gene Expression and Fucoxanthin Synthesis, Frontiers  
734 in Plant Science. 13 (2022). <https://doi.org/10.3389/fpls.2022.830069>.
- 735 [16] L. Blommaert, M.J.J. Huysman, W. Vyverman, J. Lavaud, K. Sabbe, Contrasting NPQ  
736 dynamics and xanthophyll cycling in a motile and a non-motile intertidal benthic diatom,  
737 Limnol. Oceanogr. 62 (2017) 1466–1479. <https://doi.org/10.1002/lno.10511>.
- 738 [17] B. Lepetit, G. Gélin, M. Lepetit, S. Sturm, S. Vugrinec, A. Rogato, P.G. Kroth, A.  
739 Falciatore, J. Lavaud, The diatom *Phaeodactylum tricorutum* adjusts nonphotochemical  
740 fluorescence quenching capacity in response to dynamic light via fine-tuned Lhcx and  
741 xanthophyll cycle pigment synthesis, New Phytol. 214 (2016) 205–218.  
742 <https://doi.org/10.1111/nph.14337>.

- 743 [18] P. Müller, X.-P. Li, K.K. Niyogi, Non-Photochemical Quenching. A Response to Excess  
744 Light Energy, *Plant Physiology*. 125 (2001) 1558–1566.  
745 <https://doi.org/10.1104/pp.125.4.1558>.
- 746 [19] S. Schaller-Laudel, D. Volke, M. Redlich, M. Kansy, R. Hoffmann, C. Wilhelm, R. Goss,  
747 The diadinoxanthin diatoxanthin cycle induces structural rearrangements of the isolated  
748 FCP antenna complexes of the pennate diatom *Phaeodactylum tricorutum*, *Plant*  
749 *Physiology and Biochemistry*. 96 (2015) 364–376.  
750 <https://doi.org/10.1016/j.plaphy.2015.09.002>.
- 751 [20] C. Fufezan, D. Simionato, T. Morosinotto, Identification of Key Residues for pH  
752 Dependent Activation of Violaxanthin De-Epoxidase from *Arabidopsis thaliana*, *PLOS*  
753 *ONE*. 7 (2012) e35669. <https://doi.org/10.1371/journal.pone.0035669>.
- 754 [21] M. Havaux, K.K. Niyogi, The violaxanthin cycle protects plants from photooxidative  
755 damage by more than one mechanism, *Proc Natl Acad Sci U S A*. 96 (1999) 8762–8767.
- 756 [22] H.Y. Yamamoto, T.O.M. Nakayama, C.O. Chichester, Studies on the light and dark  
757 interconversions of leaf xanthophylls, *Archives of Biochemistry and Biophysics*. 97  
758 (1962) 168–173. [https://doi.org/10.1016/0003-9861\(62\)90060-7](https://doi.org/10.1016/0003-9861(62)90060-7).
- 759 [23] P. Kuczynska, M. Jemiola-Rzeminska, K. Strzalka, Photosynthetic Pigments in Diatoms,  
760 *Marine Drugs*. 13 (2015) 5847–5881. <https://doi.org/10.3390/md13095847>.
- 761 [24] P. Kuczynska, M. Jemiola-Rzeminska, B. Nowicka, A. Jakubowska, W. Strzalka, K.  
762 Burda, K. Strzalka, The xanthophyll cycle in diatom *Phaeodactylum tricorutum* in  
763 response to light stress, *Plant Physiology and Biochemistry*. 152 (2020) 125–137.  
764 <https://doi.org/10.1016/j.plaphy.2020.04.043>.
- 765 [25] M. Lohr, C. Wilhelm, Algae displaying the diadinoxanthin cycle also possess the  
766 violaxanthin cycle, *Proceedings of the National Academy of Sciences*. 96 (1999) 8784–  
767 8789. <https://doi.org/10.1073/pnas.96.15.8784>.
- 768 [26] R. Gonçalves de Oliveira-Júnior, R. Grougnet, P.-E. Bodet, A. Bonnet, E. Nicolau, A.  
769 Jebali, J. Rumin, L. Picot, Updated pigment composition of *Tisochrysis lutea* and  
770 purification of fucoxanthin using centrifugal partition chromatography coupled to flash  
771 chromatography for the chemosensitization of melanoma cells, *Algal Research*. 51 (2020)  
772 102035. <https://doi.org/10.1016/j.algal.2020.102035>.
- 773 [27] A. Malnoë, Photoinhibition or photoprotection of photosynthesis? Update on the (newly  
774 termed) sustained quenching component qH, *Environmental and Experimental Botany*.  
775 154 (2018) 123–133. <https://doi.org/10.1016/j.envexpbot.2018.05.005>.
- 776 [28] T. Lacour, M. Babin, J. Lavaud, Diversity in Xanthophyll Cycle Pigments Content and  
777 Related Nonphotochemical Quenching (NPQ) Among Microalgae: Implications for  
778 Growth Strategy and Ecology, *Journal of Phycology*. 56 (2020) 245–263.  
779 <https://doi.org/10.1111/jpy.12944>.
- 780 [29] T. Lacour, J. Larivière, J. Ferland, F. Bruyant, J. Lavaud, M. Babin, The Role of Sustained  
781 Photoprotective Non-photochemical Quenching in Low Temperature and High Light  
782 Acclimation in the Bloom-Forming Arctic Diatom *Thalassiosira gravida*, *Frontiers in*  
783 *Marine Science*. 5 (2018). <https://www.frontiersin.org/article/10.3389/fmars.2018.00354>  
784 (accessed May 6, 2022).
- 785 [30] J. Lavaud, R. Goss, The Peculiar Features of Non-Photochemical Fluorescence Quenching  
786 in Diatoms and Brown Algae, in: *Non-Photochemical Quenching and Energy Dissipation*  
787 *in Plants, Algae and Cyanobacteria*, 2014: pp. 421–443. [https://doi.org/10.1007/978-94-017-9032-1\\_20](https://doi.org/10.1007/978-94-017-9032-1_20).
- 789 [31] K. Loubière, E. Olivo, G. Bougaran, J. Pruvost, R. Robert, J. Legrand, A new  
790 photobioreactor for continuous microalgal production in hatcheries based on external-loop  
791 airlift and swirling flow, *Biotechnology and Bioengineering*. 102 (2009) 132–147.  
792 <https://doi.org/10.1002/bit.22035>.

- 793 [32] L. Van Heukelem, C.S. Thomas, Computer-assisted high-performance liquid  
794 chromatography method development with applications to the isolation and analysis of  
795 phytoplankton pigments, *Journal of Chromatography A*. 910 (2001) 31–49.  
796 [https://doi.org/10.1016/S0378-4347\(00\)00603-4](https://doi.org/10.1016/S0378-4347(00)00603-4).
- 797 [33] J. Berthelie, N. Casse, N. Daccord, V. Jamilloux, B. Saint-Jean, G. Carrier, Annotation  
798 of the genome assembly (version 2) of the microalga *Tisochrysis lutea*, (2018).  
799 <https://doi.org/10.17882/52231>.
- 800 [34] S.F. Altschul, W. Gish, W. Miller, E.W. Myers, D.J. Lipman, Basic local alignment search  
801 tool, *Journal of Molecular Biology*. 215 (1990) 403–410. [https://doi.org/10.1016/S0022-2836\(05\)80360-2](https://doi.org/10.1016/S0022-2836(05)80360-2).
- 802 [35] W. Arsalane, B. Rousseau, J.-C. Duval, Influence of the Pool Size of the Xanthophyll  
803 Cycle on the Effects of Light Stress in a Diatom: Competition Between Photoprotection  
804 and Photoinhibition, *Photochemistry and Photobiology*. 60 (1994) 237–243.  
805 <https://doi.org/10.1111/j.1751-1097.1994.tb05097.x>.
- 806 [36] M. Lohr, C. Wilhelm, Xanthophyll synthesis in diatoms: quantification of putative  
807 intermediates and comparison of pigment conversion kinetics with rate constants derived  
808 from a model, *Planta*. 212 (2001) 382–391. <https://doi.org/10.1007/s004250000403>.
- 809 [37] K.J.M. Mulders, Y. Weesepeel, P.P. Lamers, J.-P. Vincken, D.E. Martens, R.H. Wijffels,  
810 Growth and pigment accumulation in nutrient-depleted *Isochrysis aff. galbana* T-ISO, *J*  
811 *Appl Phycol*. 25 (2013) 1421–1430. <https://doi.org/10.1007/s10811-012-9954-6>.
- 812 [38] K.J. Flynn, M. Zapata, J.L. Garrido, H. Öpik, C.R. Hipkin, Changes in carbon and nitrogen  
813 physiology during ammonium and nitrate nutrition and nitrogen starvation in *Isochrysis*  
814 *galbana*, *European Journal of Phycology*. 28 (1993) 47–52.  
815 <https://doi.org/10.1080/09670269300650071>.
- 816 [39] S. Takaichi, M. Mochimaru, Carotenoids and carotenogenesis in cyanobacteria: unique  
817 ketocarotenoids and carotenoid glycosides, *Cell. Mol. Life Sci*. 64 (2007) 2607.  
818 <https://doi.org/10.1007/s00018-007-7190-z>.
- 819 [40] C. Punginelli, A. Wilson, J.-M. Routaboul, D. Kirilovsky, Influence of zeaxanthin and  
820 echinenone binding on the activity of the Orange Carotenoid Protein, *Biochimica et*  
821 *Biophysica Acta (BBA) - Bioenergetics*. 1787 (2009) 280–288.  
822 <https://doi.org/10.1016/j.bbabi.2009.01.011>.
- 823 [41] A. Wilson, G. Ajlani, J.-M. Verbavatz, I. Vass, C.A. Kerfeld, D. Kirilovsky, A Soluble  
824 Carotenoid Protein Involved in Phycobilisome-Related Energy Dissipation in  
825 Cyanobacteria, *Plant Cell*. 18 (2006) 992–1007. <https://doi.org/10.1105/tpc.105.040121>.
- 826 [42] T. Kay Holt, D.W. Krogmann, A carotenoid-protein from cyanobacteria, *Biochimica et*  
827 *Biophysica Acta (BBA) - Bioenergetics*. 637 (1981) 408–414.  
828 [https://doi.org/10.1016/0005-2728\(81\)90045-1](https://doi.org/10.1016/0005-2728(81)90045-1).
- 829 [43] Y. Kusama, S. Inoue, H. Jimbo, S. Takaichi, K. Sonoike, Y. Hihara, Y. Nishiyama,  
830 Zeaxanthin and Echinenone Protect the Repair of Photosystem II from Inhibition by  
831 Singlet Oxygen in *Synechocystis* sp. PCC 6803, *Plant and Cell Physiology*. 56 (2015)  
832 906–916. <https://doi.org/10.1093/pcp/pcv018>.
- 833 [44] S.B.B. Mohamad, Y.A. Yousef, T.-B. Melø, T. Jávorfí, V. Partali, H.-R. Sliwka, K. Razi  
834 Naqvi, Singlet oxygen quenching by thione analogues of canthaxanthin, echinenone and  
835 rhodoxanthin, *Journal of Photochemistry and Photobiology B: Biology*. 84 (2006) 135–  
836 140. <https://doi.org/10.1016/j.jphotobiol.2006.02.006>.
- 837 [45] B. Lepetit, D. Volke, M. Gilbert, C. Wilhelm, R. Goss, Evidence for the Existence of One  
838 Antenna-Associated, Lipid-Dissolved and Two Protein-Bound Pools of Diadinoxanthin  
839 Cycle Pigments in Diatoms, *Plant Physiology*. 154 (2010) 1905–1920.  
840 <https://doi.org/10.1104/pp.110.166454>.
- 841



- 842 [46] R. Goss, B. Lepetit, Biodiversity of NPQ, *Journal of Plant Physiology*. 172 (2015) 13–32.  
843 <https://doi.org/10.1016/j.jplph.2014.03.004>.
- 844 [47] L. Blommaert, L. Chafai, B. Bailleul, The fine-tuning of NPQ in diatoms relies on the  
845 regulation of both xanthophyll cycle enzymes, *Sci Rep*. 11 (2021) 12750.  
846 <https://doi.org/10.1038/s41598-021-91483-x>.
- 847 [48] T. Jakob, R. Goss, C. Wilhelm, Unusual pH-dependence of diadinoxanthin de-epoxidase  
848 activation causes chlororespiratory induced accumulation of diatoxanthin in the diatom  
849 *Phaeodactylum tricorutum*, *Journal of Plant Physiology*. 158 (2001) 383–390.  
850 <https://doi.org/10.1078/0176-1617-00288>.
- 851 [49] G. Yellen, The voltage-gated potassium channels and their relatives, *Nature*. 419 (2002)  
852 35–42. <https://doi.org/10.1038/nature00978>.
- 853 [50] E.E. Pfundel, R.A. Dilley, The pH Dependence of Violaxanthin Deepoxidation in Isolated  
854 Pea Chloroplasts, *Plant Physiology*. 101 (93) 65–71. <https://doi.org/10.1104/pp.101.1.65>.
- 855 [51] J. Lavaud, A.C. Materna, S. Sturm, S. Vugrinec, P.G. Kroth, Silencing of the Violaxanthin  
856 De-Epoxidase Gene in the Diatom *Phaeodactylum tricorutum* Reduces Diatoxanthin  
857 Synthesis and Non-Photochemical Quenching, *PLOS ONE*. 7 (2012) e36806.  
858 <https://doi.org/10.1371/journal.pone.0036806>.
- 859 [52] Y. Bai, T. Cao, O. Dautermann, P. Buschbeck, M.B. Cantrell, Y. Chen, C.D. Lein, X. Shi,  
860 M.A. Ware, F. Yang, H. Zhang, L. Zhang, G. Peers, X. Li, M. Lohr, Green diatom mutants  
861 reveal an intricate biosynthetic pathway of fucoxanthin, *Proc. Natl. Acad. Sci. U.S.A.* 119  
862 (2022) e2203708119. <https://doi.org/10.1073/pnas.2203708119>.
- 863 [53] R. Goss, E. Ann Pinto, C. Wilhelm, M. Richter, The importance of a highly active and  
864  $\Delta$ pH-regulated diatoxanthin epoxidase for the regulation of the PS II antenna function in  
865 diadinoxanthin cycle containing algae, *Journal of Plant Physiology*. 163 (2006) 1008–  
866 1021. <https://doi.org/10.1016/j.jplph.2005.09.008>.
- 867 [54] K.K. Niyogi, T.B. Truong, Evolution of flexible non-photochemical quenching  
868 mechanisms that regulate light harvesting in oxygenic photosynthesis, *Current Opinion in*  
869 *Plant Biology*. 16 (2013) 307–314. <https://doi.org/10.1016/j.pbi.2013.03.011>.
- 870 [55] J.M. Buck, J. Sherman, C.R. Bártulos, M. Serif, M. Halder, J. Henkel, A. Falciatore, J.  
871 Lavaud, M.Y. Gorbunov, P.G. Kroth, P.G. Falkowski, B. Lepetit, LhcX proteins provide  
872 photoprotection via thermal dissipation of absorbed light in the diatom *Phaeodactylum*  
873 *tricorutum*, *Nature Communications*. 10 (2019) 4167. <https://doi.org/10.1038/s41467-019-12043-6>.
- 875 [56] M. Nymark, K.C. Valle, T. Brembu, K. Hancke, P. Winge, K. Andresen, G. Johnsen, A.M.  
876 Bones, An Integrated Analysis of Molecular Acclimation to High Light in the Marine  
877 Diatom *Phaeodactylum tricorutum*, *PLOS ONE*. 4 (2009) e7743.  
878 <https://doi.org/10.1371/journal.pone.0007743>.
- 879 [57] L. Taddei, G.R. Stella, A. Rogato, B. Bailleul, A.E. Fortunato, R. Annunziata, R. Sanges,  
880 M. Thaler, B. Lepetit, J. Lavaud, M. Jaubert, G. Finazzi, J.-P. Bouly, A. Falciatore,  
881 Multisignal control of expression of the LHCX protein family in the marine diatom  
882 *Phaeodactylum tricorutum*, *EXBOTJ*. 67 (2016) 3939–3951.  
883 <https://doi.org/10.1093/jxb/erw198>.
- 884 [58] J. Lavaud, R.F. Strzepek, P.G. Kroth, Photoprotection capacity differs among diatoms:  
885 Possible consequences on the spatial distribution of diatoms related to fluctuations in the  
886 underwater light climate, *Limnology and Oceanography*. 52 (2007) 1188–1194.  
887 <https://doi.org/10.4319/lo.2007.52.3.1188>.
- 888 [59] D. Croteau, T. Lacour, N. Schiffrine, P.-I. Morin, M.-H. Forget, F. Bruyant, J. Ferland, A.  
889 Lafond, D.A. Campbell, J.-E. Tremblay, M. Babin, J. Lavaud, Shifts in growth light  
890 optima among diatom species support their succession during the spring bloom in the

891 Arctic, *Journal of Ecology*. 110 (2022) 1356–1375. <https://doi.org/10.1111/1365->  
892 2745.13874.  
893 [60] A. Barnett, V. Méléder, L. Blommaert, B. Lepetit, P. Gaudin, W. Vyverman, K. Sabbe, C.  
894 Dupuy, J. Lavaud, Growth form defines physiological photoprotective capacity in  
895 intertidal benthic diatoms, *ISME J.* 9 (2015) 32–45.  
896 <https://doi.org/10.1038/ismej.2014.105>.  
897